



CAV site-effect assessment: A case study of Taipei Basin

J.P. Wang^{a,*}, Xu Yun^b, H. Kuo-Chen^c, Yih-Min Wu^d

^a Department of Civil Engineering, National Central University, Taiwan

^b Department of Civil and Environmental Engineering, Hong Kong University of Science and Technology, Hong Kong

^c Department of Earth Sciences, National Central University, Taiwan

^d Department of Geosciences, National Taiwan University, Taiwan

ARTICLE INFO

Keywords:

Cumulative absolute velocity (CAV)

Site effect

Taipei

ABSTRACT

Recent studies have shown that structural damage exhibits stronger correlations with cumulative absolute velocity (CAV) than other ground motion intensity measures (e.g., PGA). This paper presents a CAV site-effect assessment for the Taipei areas for the first time. The study was based on more than 1200 strong-motion data from 47 major earthquakes that had occurred around Taiwan. The results show that the site effects are more conspicuous in the western Taipei than the eastern areas, and it is also obvious that the site effect is strong in locations close to the rims of the basin, where seismic waves could be easily reflected, refracted and super-imposed. Subsequently, a map showing the areas in Taipei subject to severe CAV amplification and/or high variability was developed for site-effect microzonation for the study area, on the basis of CAV that was considered better correlated with structural damage under earthquake condition.

1. Introduction

In an attempt to avoid unnecessary post-earthquake shutdowns of nuclear power plants for safety inspection, in the 1980s the Electric Power Research Institute (EPRI) proposed a new ground motion intensity measure called cumulative absolute velocity (CAV). It considers a motion's amplitude, duration and waveform altogether. Fig. 1(a) illustrates the CAV of a hypothetical ground motion, which is calculated as follows [1]:

$$CAV = \int_0^{t_{\max}} |a(t)| dt \quad (1)$$

where $|a(t)|$ is the absolute value of acceleration at time t , while t_{\max} denotes the total duration of the acceleration time history.

The EPRI study also highlighted that among different intensity measures, CAV correlates most strongly with MMI VII (Modified Mercalli intensity scale VII) that describes the onset of structural damage. EPRI further suggested 0.3 g-s as the CAV threshold that could cause damage on the structures with good design and construction [1]. Subsequently, considering small-amplitude motions are unlikely to cause structural damage, several variants (denoted as CAV') were proposed by containing only larger-amplitude motions (e.g., [2–5]):

$$CAV' = \sum_{i=1}^N H(pga_i - pga_{\text{threshold}}) \int_{t=t_i}^{t=t_{i+1}} |a(t)| dt \quad (2)$$

where N is the total duration of a ground motion in seconds, pga_i is the maximum acceleration (absolute value) in the i -th second of the motion, $pga_{\text{threshold}}$ is the acceleration threshold, and $H(x)$ is the Heaviside function:

$$H(x) = \begin{cases} 1, & x \geq 0 \\ 0, & x < 0 \end{cases} \quad (3)$$

For example, CAV_5 and CAV_{20} that have been proposed are the summation of those one-second intervals with PGA above 0.005 g and 0.02 g, respectively [3,4]. Fig. 1(b) is a schematic diagram demonstrating such CAV variants graphically.

After the new intensity measure was proposed, a variety of CAV research was reported, such as the correlations between CAV and structural safety/damage. For example, Cabañas et al. [4] found that CAV_{20} had a strong correlation with the local macro-seismic intensity (also known as MSK) in Italy that was developed based on the degrees of structural damages. Using the PEER-NGA (Pacific Earthquake Engineering Research Center; Next Generation Attenuation) strong-motion database, Campbell and Bozorgnia [5] were able to characterize a CAV threshold by comparing CAV levels that caused structural damage with the JMA (Japan Meteorological Agency) intensity scale.

Other CAV-related studies include the developments of CAV ground motion prediction equations (GMPEs) (e.g., [6–9]). For instance, Campbell and Bozorgnia [8] developed several CAV GMPEs based on the PEER-NGA database, and pointed out the aleatory uncertainty

* Corresponding author.

E-mail address: jpwang@ncu.edu.tw (J.P. Wang).

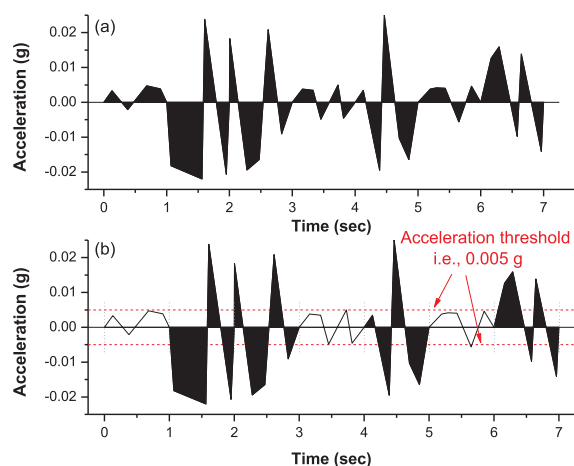


Fig. 1. Illustration of CAV (the shaded areas) with a hypothetical acceleration time history: (a) CAV; (b) CAV_5 .

associated with the CAV GMPEs was lower than that of PGA GMPEs. (It implies CAV is better correlated with earthquake magnitude and distance than PGA.) Note that prior to the CAV GMPE study, Campbell and Bozorgnia [11] indicated the smallest standard deviations were those for PGA, PGV, and PSA with period ≤ 0.02 s, among a number of GMPEs they developed for PGA, PGV, and 5% damped response spectra for periods ranging from 0.01 to 10 s.

New applications of CAV to earthquake engineering were also proposed after the new intensity measure appeared. On the basis of probabilistic seismic hazard analysis (PSHA) that calculates the annual rate of PGA exceedance at a site of interest, the so-called “CAV-filtered PSHA” was proposed [10] in terms of both PGA and CAV exceedances (e.g., $PGA > 0.2$ g and $CAV > 0.16$ g-s). Understandably, the objective of the new assessment is to make the hazard estimates more relevant to structural damage with CAV taken into account, unlike the conventional ones solely depending on PGA exceedance. On the other hand, Kramer and Mitchell [3] studied soil liquefaction and its correlation with different intensity measures, and recommended CAV_5 for soil liquefaction assessment because of its strongest correlation with pore pressure generation in soil. In earthquake early warning, Alcik et al. [12] proposed a new system that will be activated based on the CAV of early ground motions that have been detected, different than the existing systems based on the amplitudes of early motions.

It has been noted that the duration of strong ground motion is also well correlated with earthquake damage. Several physical process, such as strength degradation of certain structures, are sensitive to the number of load (or stress reversals) present in earthquake motions. That is, unlike a long-duration ground motion, a short-duration motion might not be able to produce adequate stress reversals to cause structural damage [33]. More specifically, Bray and Rathje [34] pointed out a landfill's permanent base displacement induced by earthquakes is governed by duration along with a few key factors. Hancock and Bommer [35] considered the duration of ground motion was well correlated with fatigue damage for an 8-storey RC wall-frame building. Chandramohan et al. [36] found that the collapse capacity of concrete bridge piers subject to long-duration motions would be 17% lower than that when they are subject to short-duration motions, and such a finding echoes the study of Raghunandan and Liel [37] concluding ground motion duration plays an important role in the collapse resistance of structures.

Nevertheless, very few studies were reported about the correlation between CAV and duration. Based on earthquake records around Greece, Koliopoulos et al. [7] investigated the respective regression between MMI (Modified Mercalli Intensity) and PGA, CAV, bracketed duration with zero cutoff (BDO), etc. They found that the R^2 value of the MMI-CAV regression was close to that of the MMI-BDO regression (both

greater than that of the MMI-PGA regression), which indirectly shows CAV and such a duration measure could be closely related, with both having good correlation with MMI based on the level of structural damage.

Site effect is also one of the key topics in earthquake studies (e.g., [13–19]), especially for places sitting on thick layers of (soft) soils like the city of Taipei. As a result, a series of site-effect studies have been conducted for the city (the most important city in Taiwan) since the 1990s (e.g., [16–21]). Based on the data from three major earthquakes, Wen et al. [16] found that the areas along two rivers in the Taipei areas were more susceptible to site amplification, and pointed out the degree of site effect could vary substantially upon the frequency content of the incident bedrock motion. Similarly, by analyzing earthquake data from a shallow earthquake (focal depth of 5.3 km) and from a deep earthquake (focal depth of 39.8 km), Loh et al. [18] concluded that shallow earthquakes should be able to cause stronger site effects in Taipei than deep earthquakes. Sokolov et al. [19] further provided the rationale behind those findings, considering the site effects in Taipei should be mainly related to the thicknesses of soil layers, bedrock topography, and the degrees of irregularities and complexities on the rims of the basin.

Nevertheless, the site-effect studies summarized above were all PGA- or SA-based (SA: spectral acceleration), not in terms of CAV that is now being considered more indicative of structural damage. In addition, the previous studies based on limited data were unable to investigate the variability inherent in site effect owing to the high levels of earthquake randomness.

The key scope of this study is to conduct the first CAV site-effect assessment for Taipei. More than 1200 strong-motion data were first collected, based on which the site effect and its variability were investigated. The geological backgrounds of the study area and the data mining process were also introduced in the paper.

2. Geological background of the Taipei Basin

As shown in Fig. 2(b), the Taipei Basin in northern Taiwan is surrounded by the Tatun Volcano Group in the north, the Kuanyin Mountain and Linkou Tableland in the west, and the Western Foothills in the south and east. The basin has a total area of about 240 km², and is 2–20 m above the sea level. According to the Central Geological Survey of Taiwan (CGST), the bedrock of the Taipei Basin is mainly made up of Tertiary sedimentary rock. Above the bedrock, the basin was filled with unconsolidated Quaternary sediments, forming the Hsinchuang Formation, Chingmei Formation, and the Sungshan Formation [22].

The Taipei Basin gradually took shape owing to the evolutions of the Shanchiao Fault in the west. As shown in Fig. 2(c), the western parts of Taipei that lie along the fault have accumulated thicker sediments than in the eastern parts [22,23], resulting in an asymmetrical soil profile/thickness across the basin. Beginning in the west, the Quaternary sediments above the bedrock can be 500- to 600-meter thick, with the thickness attenuating toward the southeast (Fig. 2(b)).

3. Taiwan Strong Motion Instrumentation Program (TSMIP)

Taiwan is located in a region known for high seismicity, and the Taiwan Strong Motion Instrumentation Program (TSMIP) was launched in the 1990s to collect high-quality seismic data for earthquake research. TSMIP currently has 688 free-field seismic stations (Fig. 3), constituting a “high-density” earthquake instrumentation network in Taiwan [24]. Each station has accelerometers to record earthquake motions in three directions with a sampling rate of 200 or 250 per second [25]. Of all the stations, about 100 are equipped with automatic data transmitting systems that facilitate real-time analyses [26]. According to the latest report, the seismic stations were further categorized as a hard-rock site, rock site, soft-rock site, stiff-soil site, or soft-soil site. For more details on these site characterizations, refer to Kuo et al.

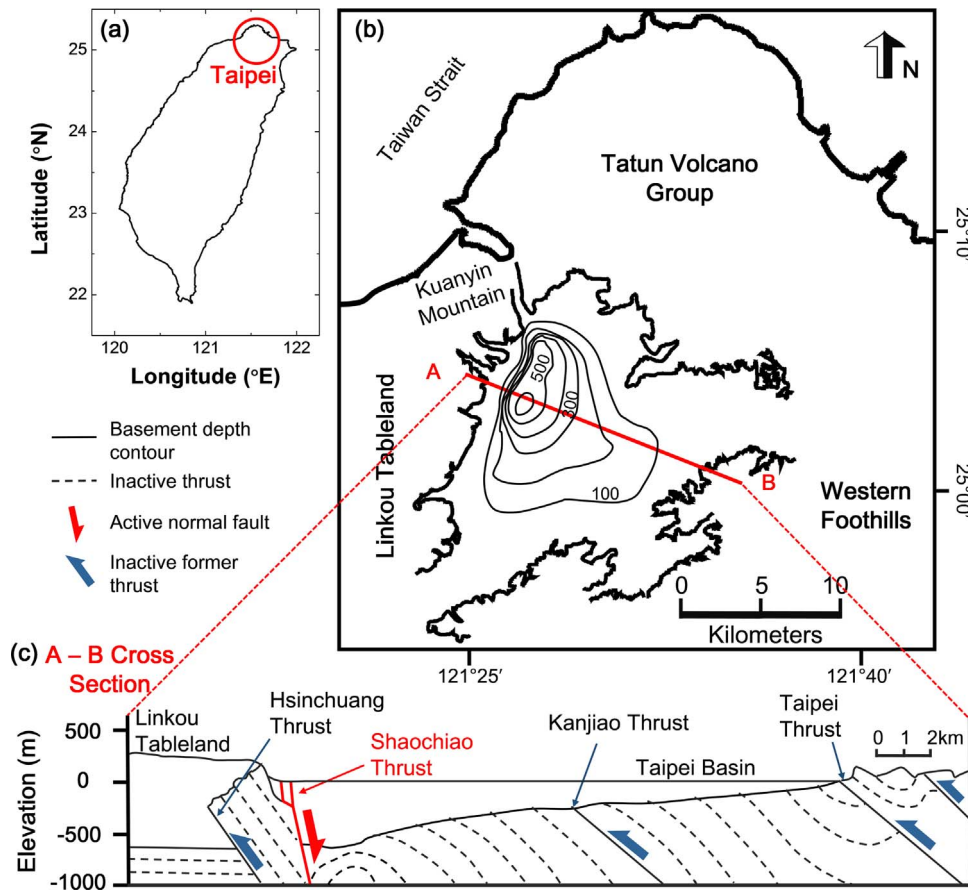


Fig. 2. (a) Location of the Taipei Basin in northern Taiwan; (b) Boundary of the basin and the contours of soil thickness; and (c) The E-W cross section of the Taipei Basin (after Wang et al. [23]).

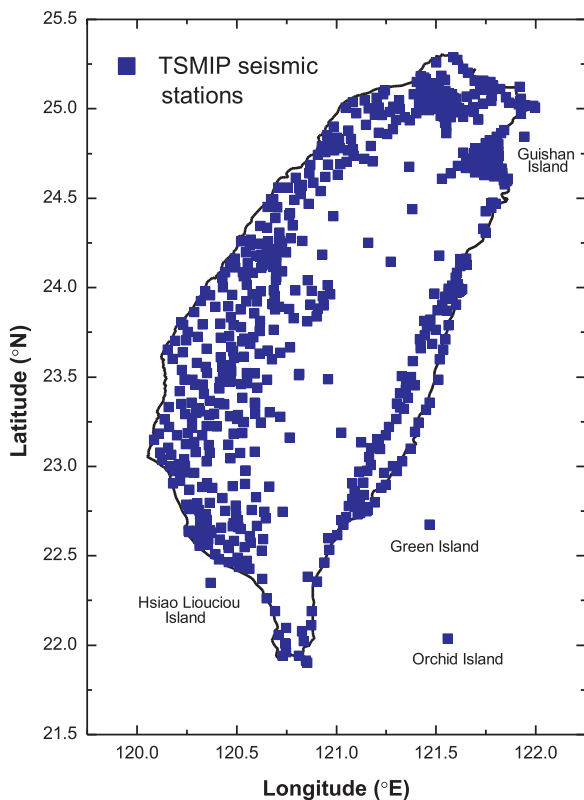


Fig. 3. Locations of the 688 free-field seismic stations of TSMIP [25].

[27].

Additional information regarding TSMIP is given in this section mainly based on the National Center for Research on Earthquake Engineering (NCREE) of Taiwan [39] that is responsible for the establishment of TSMIP. Since its establishment, about 10 different models of seismometers have been installed in TSMIP stations, from the early 12-bit-resolution models to the recent 24-bit-resolution ones. All the seismometers are acceleration types that record acceleration time histories directly. The seismometers will be in action when they detect a single greater than 3.9 gal, and then retrieve the records of the last 20 s backward. Currently, GPS (global positioning system) has been installed in most stations for time calibration. Based on NCREE, the TSMIP personnel will go to the site every three months to gather the data stored in the computer of the seismic station. Nonetheless, the information regarding the site noise (mainly resulting from installation and site condition) and the instrument noise (from the machine itself) was not given in the report.

According to Boore [40], the processing of strong motion data are generally about baseline corrections, filtering acceleration time histories and integrating them for calculating velocity and displacement time histories. Since the sampling rate of the seismographs of TSMIP is 200/250 per second, the baseline correction is not necessarily needed [41]; therefore, two major steps in processing the raw data of acceleration time history are as follows: 1) the zeroth-order correction was performed by subtracting the mean of the pre-event portion from the whole trace, which is the mandatory procedure in processing acceleration records [42]; 2) zero pads are appended to both the beginning and the end of the recorded data, given zero reading on the two ends being the presumption in time-domain filtering programs [40]. Converse and Brady [43] recommended the pad length could be determined

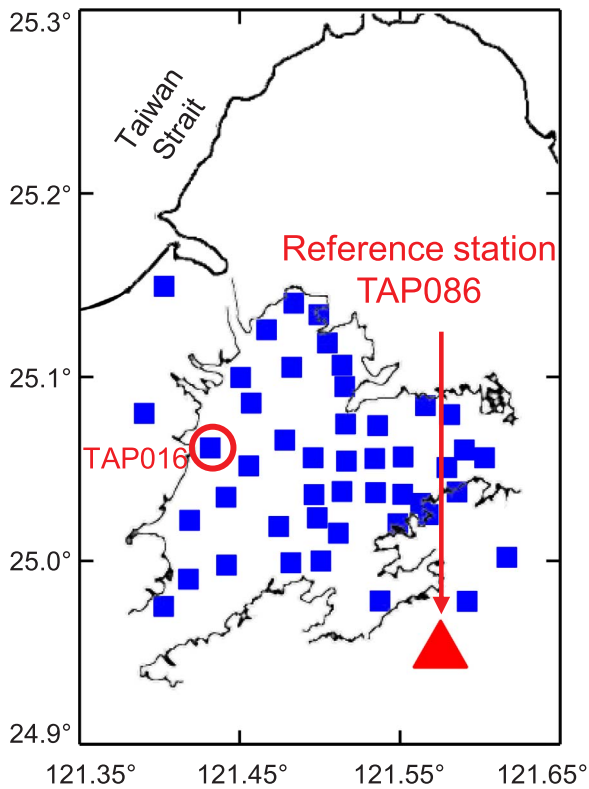


Fig. 4. Locations of the 47 seismic stations in the study area; TAP086 was used as the reference site in this study, while TAP016 that was used in previous site-effect investigations was chosen for the sensitivity study present herein.

from the following formula:

$$Tz_{pad} = 1.5 \times n/f_c \quad (4)$$

where Tz_{pad} is the total length of the zero pads to be added (half length of the zeros added to the beginning of the original data and the other half added to the end of the original data); n is the order of the Butterworth filter; f_c is the cutoff frequency. To be more specific, the high-pass Butterworth filter was applied with the cutoff frequency set at 0.075 Hz according to studies that also had to conduct TSMIP-data processing prior to an application (e.g., [38,44]).

Since the establishment of TSMIP, the database has been used in several studies (e.g., [28–31]). For example, Lin et al. [30] used it to develop the first series of local GMPEs (including PGA, 1-Hz SA, 5-Hz SA, etc.), which helped refine seismic hazard studies for the region around Taiwan [32].

This present study is also based on the TSMIP database. Fig. 4 shows the 47 stations that are located in and near the Taipei Basin. Therefore, the first task is to collect data of the 47 stations from the TSMIP database. In total, 1226 ground motions associated with 47 major earthquakes above M_L 5.0 (Table 1) were gathered. After data mining, the next task is to compute the CAV of the 1226 motions. Clearly, an in-house toolbox was developed for such repetitive computation. It is noting that, compared to the previous works, the sample size of this study is much larger for such a site-effect investigation.

4. Basin effect analysis

4.1. CAV ratio calculation

Based on the records of acceleration time histories, the approach employed in this CAV study is similar to the aforementioned site-effect, empirical studies for Taipei [16–19]. Specifically, the analysis of this study is similar to the so-called “spectral ratio method” that computes

the SA ratio of ground surface motion to bedrock motion. Although this study computes CAV ratios instead of PGA or SA ratios, the local site effect is considered in existence when the ratio is greater than one, either based on amplitude-based intensity measures like PGA, or based on “integrated” intensity measures like CAV. It is noted that the key presumption of the analysis is that the waveform of ground motions propagating from distant sources to the Taipei Basin should be more or less the same irrespective of the bedrock location, especially when it comes to far-field earthquakes like the 47 events analyzed with epicentral distances ranging from 65 to 210 km.

It is noted that Sokolov et al. [19] adopted a similar approach to study the local site effect in Taipei also based on ground motion records. However, instead of using rock outcropping motions at a reference site and considering them as bedrock motions, they used local GMPEs that were newly developed to calculate the theoretical PGA and SA of bedrock motions at a hypothetical reference site. They claimed that this approach can increase the sample size for such analysis because a reference site is not needed. Nonetheless, the approach is not applicable to this study because CAV GMPEs for Taiwan regions have not yet been developed. In other words, the CAV of bedrock motion is not attainable from such a theoretical calculation without a local CAV GMPE. On the other hand, considering the study area is relatively small and far-field earthquakes are the main sources of ground motion records that were analyzed, the difference in distance between source-to-outcrop (at a reference site) and source-to-bedrock (under the site of interest) should be less than few kilometers, resulting in a negligible CAV estimation between the two approaches.

Using the first approach, the first step of the analyses is to determine the best reference site. In this study, Station TAP086 (see Fig. 4) was used as the reference site, which was built on a rock site with a Vs_{30} of 943 m/s [24]. (Vs_{30} : average shear-wave velocity of soil/rock 30 m below the ground surface.) More discussions on reference sites will be given in one following section.

Unlike site-specific ground response analysis with detailed site characterizations (e.g., soil profile, layer thickness, shear-wave velocity, soil unit weight and shear modulus), it is understood that such an approach/analysis present herein is to provide an overview on the site effect of a study area. Therefore, the scope of such a regional study is quite different from a site-specific investigation that aims to develop site-specific design parameters like ground motion response spectra.

4.2. Results

Fig. 5 shows the result of the analysis. The values in the map are the average of the 47 CAV amplification ratios based on the strong-motion data induced by 47 major earthquakes (Table 1). It shows the site effects are more severe in western Taipei (Zone A in Fig. 5) than in eastern Taipei (Zone C in Fig. 5), with the average CAV amplification ratio around 1.5–2 and 1–1.5, respectively. As indicated by previous studies, this should be attributed to the thicknesses of soil layers that were unevenly distributed in the study area (see Fig. 2).

The analysis also shows that the average CAV ratio can be quite large (about 2.0–2.5) at locations close to the rim of the basin, especially in the south and the east (Zone B in Fig. 5). Similar to the results discovered by previous PGA-based analyses, such a finding should be related to the complex and irregular geological/geographical conditions close to the rim of the basin where seismic waves could be easily refracted, reflected, and superimposed.

Fig. 6 shows the map demonstrating the level of site effect in terms of mean CAV ratio plus one standard deviation based on 47 events/analyses. In other words, this map can help identify those areas in the Taipei Basin under severe site effect and/or substantial variability. Accordingly, we found the areas close to the rims of the basin (south, east, and north) are more susceptible to CAV amplification, considering the relatively high mean ratio and variability combined.

It is worth noting that the empirical study present herein was based

Table 1
Summary of the 47 major earthquakes that generated 1226 ground motion data analyzed in this CAV-based site-effect study.

Earthquake events	Date (DD/MM/YYYY)	Magnitude (M_L)	Longitude (°E)	Latitude (°N)	Focal depth (km)
1	04/04/1999	5.82	121.56	24.53	88.95
2	07/05/1999	5.44	121.53	24.44	4.17
3	03/06/1999	6.18	122.29	24.24	61.67
4	11/07/1999	5.07	121.5	24.36	73.17
5	20/09/1999	7.3	120.48	23.51	8
6	20/09/1999	5.97	121.2	24.5	6.16
7	20/09/1999	6.44	121.2	23.54	7.68
8	20/09/1999	6.7	121.4	23.51	12.49
9	22/09/1999	6.8	121.2	23.49	15.59
10	22/09/1999	6.2	121.1	23.45	17.38
11	25/09/1999	6.8	121	23.51	12.06
12	30/09/1999	5.53	121.59	24.42	70.55
13	01/11/1999	6.9	121.43	23.21	31.33
14	14/06/2001	6.3	121.55	24.25	17.29
15	12/02/2002	6.2	121.43	23.44	29.98
16	31/03/2002	6.8	122.11	24.8	13.81
17	15/05/2002	6.2	121.52	24.39	8.52
18	28/05/2002	6.2	122.23	23.54	15.23
19	30/05/2002	5.55	121.56	24.52	86.99
20	29/08/2002	5.19	121.48	24.48	82.93
21	07/09/2002	5.26	121.41	24.26	41.36
22	10/09/2002	5.38	122	24.52	103.54
23	10/11/2002	5.42	121.5	24.53	110.27
24	25/12/2002	5.24	121.49	24.27	55.79
25	09/06/2003	5.72	122.01	24.22	23.22
26	09/06/2003	5.03	121.51	24.22	2.36
27	10/06/2003	6.48	121.41	23.3	32.31
28	18/07/2003	5.06	121.5	24.35	74.39
29	11/08/2003	5.38	121.33	24.35	58.49
30	12/11/2003	5.39	121.57	24.27	21.29
31	29/12/2003	5.21	121.57	24.35	68.19
32	09/05/2004	5.49	121.45	24.34	69.16
33	06/07/2004	5.22	122.15	24.53	5.96
34	29/11/2005	5.51	122.02	24.45	68.04
35	09/09/2008	5.94	122.38	24.36	103.84
36	17/04/2009	5.33	121.4	23.55	43.43
37	13/07/2009	6	122.13	24.01	18.08
38	03/10/2009	6.09	121.34	23.38	29.15
39	19/12/2009	6.92	121.39	23.47	43.78
40	04/01/2010	5.46	121.49	24.11	46.05
41	30/08/2010	5.16	122.12	24.57	15.02
42	21/11/2010	6.14	121.41	23.51	46.87
43	30/04/2011	5.81	121.48	24.39	75.02
44	09/06/2012	6.62	122.18	24.27	69.88
45	17/01/2013	5.08	121.58	24.26	13.65
46	07/03/2013	5.87	121.27	24.18	5.55
47	02/06/2013	6.48	120.58	23.51	14.54

on observed ground motions, which should be the end result of nonlinear or linear site responses. As pointed out by Wen et al. [16] who also investigated the local site effect empirically (not based on CAV), the nonlinear site response should be occurring in the study area during strong earthquakes, and suggested a nonlinear dynamic analysis should be employed when it comes to an analytical study. Nonetheless, the process or mechanism of the site response should not affect an empirical study (like this study) that is based on observational records, which are the data readily available and from which the empirical findings were directly obtained. This is a fundamental difference from an analytical site response analysis/simulation governed by linear or nonlinear models that are used, for which the analytical model needs to be properly selected and justified based on the subject/purpose of a site response investigation that is carried out using analytical and theoretical approaches.

4.3. Comparison to previous PGA-based analysis

Since PGA is still an important intensity measure in earthquake engineering, two previous studies have reported earthquake-induced PGA distributions throughout the study area. According to Loh et al.

[18], it was found that larger PGA values were present at locations close to the eastern rim of the basin and the western Taipei with thicker soil layers. In addition, with the PGA of bedrock motion estimated from downhole observations in the western Taipei, they reported the PGA amplification factor, or the PGA ratio between the ground surface motion and bedrock motion (140 m below the ground surface), as 2.3 and 2.9 in the western Taipei during two major earthquakes ($M_L = 6.57$ and 6.50). However, it is noted that the study did not select a reference site for a detailed presentation on PGA ratios throughout the study area.

With the main focus on investigating the dominant frequencies throughout the Taipei Basin, Wen et al. [16] also briefly reported the PGA distributions in the study area during three earthquakes ($M_L = 5.7$, 5.4, and 6.2). They found that during the M_L 6.2 event, the maximum and minimum PGA within the study area were equal to 97 and 20 cm/s², respectively, leading to a statement in their report that “the variation of PGA is the Taipei Basin can be in a factor of 5.” However, it is noted that the ratios between the maximum and minimum PGA in the other two events were only equal to 2 and 3.4, resulting in an average PGA ratio among the three events around 3.4, which is relatively close to 2.3 and 2.9 reported by Loh et al. [18] based on two different events. Furthermore, the study found that PGA was relatively large at locations

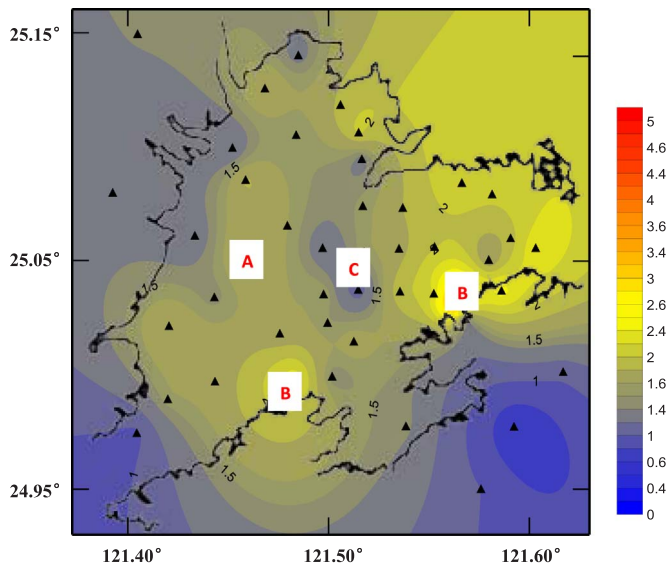


Fig. 5. Mean CAV amplification ratio with strong-motion data from 47 major earthquakes (Table 1); western Taipei (Zone A) and the locations close to the rim of the basin (Zone B) are subject to more substantial site effect, in contrast to eastern Taipei (Zone C) with less severe site effect.

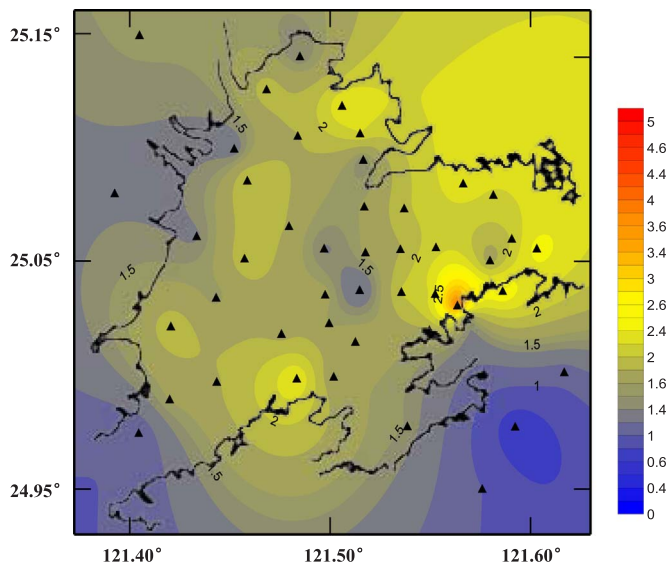


Fig. 6. Site-effect assessments for the study area; the values in the map are the mean CAV amplification ratio plus one standard deviation.

in the western Taipei due to thicker soil layers, and therefore they suggested seismic microzonation works be necessary for the study area. Nevertheless, like the study of Loh et al. [18], they did not report PGA-based amplification maps for the study area with respect to a reference site.

Comparing the two to the CAV study present herein, the similarity is that the ground surface motions throughout the study area can vary substantially, either in terms of CAV or PGA. Secondly, all the three studies (either based on CAV or PGA) indicated that thick soil layers and basin-edge effect could amplify ground surface motions more substantially. But on the other hand, it seems that the PGA ratio could be larger than the CAV ratio. Taking the western Taipei for example, the (average) PGA ratios reported in the two studies were 2.6 and 3.4, while the (average) CAV ratio estimated from this study was around 2. Although the sample size in the three studies is quite different (which might make the comparison questionable), the lower CAV ratio was somehow expectable with the nature of CAV being the combination of

low- and high-frequency motions of the whole acceleration time history. That is, for a particular site, the amplitude ratio for a particular frequency could be relatively large owing to resonance, but the CAV ratio should remain more stable for being the “average” of the large amplification at the resonant frequency, and the small to moderate amplification at other frequencies that are not close to the natural frequency of the soil column at the particular site.

4.4. Earthquake type/source on the local site effect

According to Loh et al. [18], they considered earthquakes with a substantial focal depth (referred to as deep earthquakes) should behave more like a point source; therefore, deep earthquakes could cause less variation in the local site effect in Taipei than shallow earthquakes that are governed by the complicated mechanism related to fault rupturing. In other words, shallow earthquakes should pose more threats and uncertainties on the (seismic) safety of structures owing to fault-rupturing mechanisms that involve in the genesis of shallow earthquakes.

As a result, we further divided the data into two groups. For the deep-earthquake group, it contains the data associated with earthquakes having a focal depth greater than 35 km; otherwise they are referred to as shallow-earthquake data (< 35 km). Note that the separation is based on the suggestion from Sokolov et al. [19] who also investigated the local site effect in Taipei with a hypothetical bedrock response spectra estimated with PGA and SA GMPEs.

Figs. 7 and 8 shows the mean CAV ratios calculated from deep- and shallow-earthquake data, respectively. Note that the sample size of the two groups is comparable, with 22 deep earthquakes and 25 shallow earthquakes among the pool of the data. The graphs show the spatial distribution pattern is somewhat comparable, with the locations close to the rims of the basin having relatively high CAV ratios in both cases. However, it is obvious that shallow earthquakes (Fig. 8) caused a larger CAV ratio than deep earthquakes did (Fig. 7), which is similar to the finding from Loh et al. [18] that larger PGA amplification was present during shallow earthquakes, related to the mechanism of fault rupturing that could occur near the ground surface.

5. Discussions

5.1. Reference site and sensitivity analysis

It is understood that the site-effect study is dependent on the reference site selected. In previous studies (e.g. [16–18]), Station TAP016

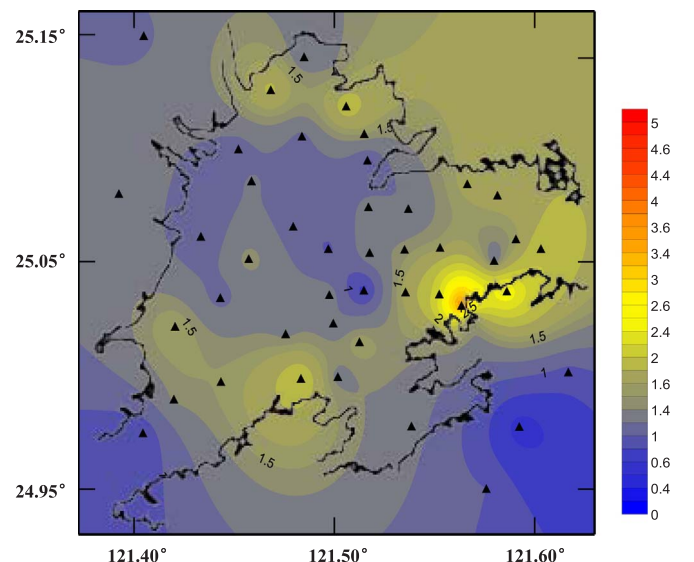


Fig. 7. Mean CAV amplification ratio associated with deep-earthquake (> 35 km) data.

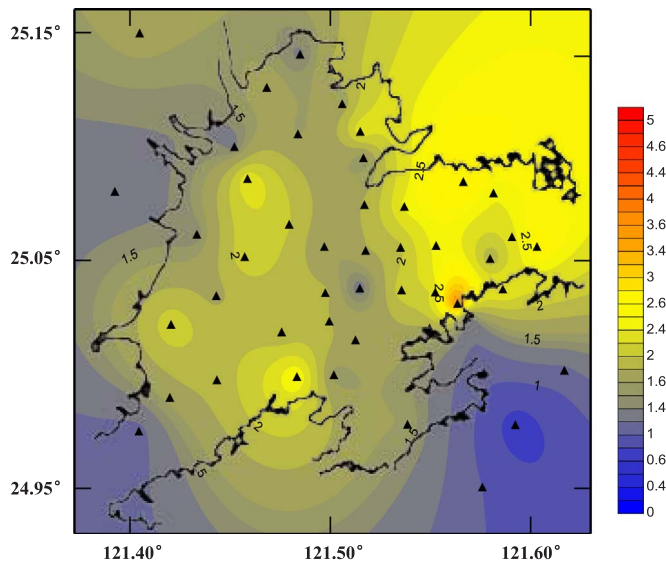


Fig. 8. Mean CAV amplification ratio associated with shallow-earthquake (< 35 km) data.

was used as the reference site, with the primary concern that its location should be able to reduce the variations of azimuth and incident angles of the seismic waves mostly from central and eastern Taiwan. However, according to the latest report [27], TAP016 has a fairly low Vs30 of 327 m/s, which makes it an unsuitable reference site that is usually a rock site or close to a rock site. As a result, in this study we used TAP086 as the reference site considering it has the largest Vs30 of 943 m/s among the 47 seismic stations around the study area.

In order to examine the influence of reference site on the site-effect assessment, we repeated the whole analyses, from data mining to the calculations, using the “old” TAP016 as the reference site adopted by the previous studies. Fig. 9 shows the result of the analysis. Comparing it to Fig. 5 using TAP086 as the reference site, we found the two are in good agreement in terms of spatial distribution patterns, while the average CAV amplification ratio in Fig. 9, using TAP016 as the reference site, is about 60–70% of those shown in Fig. 5 (using TAP086 as the reference site). As a result, this sensitivity study verified that the regional pattern of site effect should be barely affected by reference sites, while the absolute severity could be affected. The bottom line is, it is more proper to use TAP086 as a reference site as we did in this study,

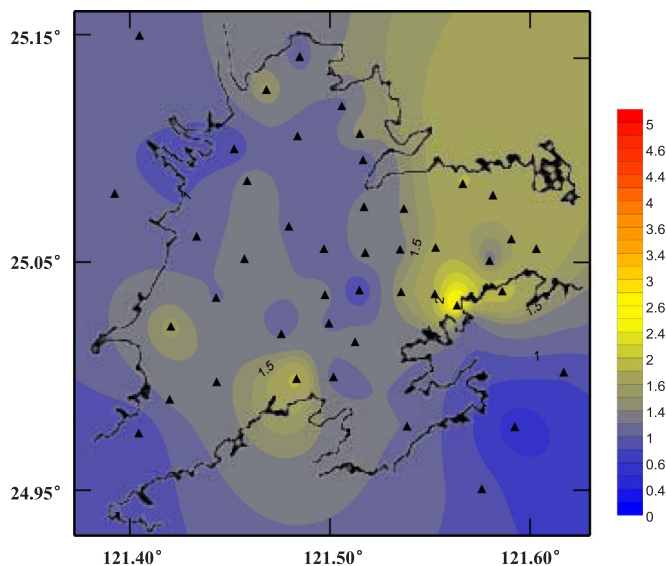


Fig. 9. Mean CAV amplification ratio using TAP016 as the reference site (see Fig. 4).

although the sensitivity study demonstrated the results between the two were not too much different in terms of the spatial distribution.

5.2. Physical interpretations on site effect

This section provides some explanations and interpretations to those areas where should be under substantial site effects based on the results of this study. The first fundamental cause should be the resonance effect between the soils and the incident waves. Specifically, the western parts and the southern borders of the basin were found having a low natural frequency of 0.5–1.5 Hz [19], causing a resonance with the incident waves mainly with low-frequency contents in that range, owing to the fact that the incident seismic waves were mostly generated by far-field earthquakes.

Second, a thicker soil layer in which seismic waves should propagate more slowly can trap more incident waves and superimpose them to cause amplification, which should be the reason that the locations in western Taipei close to the Shanchiao Fault (Fig. 2) are subjected to a more substantial site effect (Fig. 5). Furthermore, the complex and irregular geological/geographical conditions close to the rim of the basin should be able to generate similar effects for seismic waves to be easily reflected, refracted, and superimposed at those boundaries, and therefore result in a substantial amplification or strong site effect.

5.3. Microzonation

As mentioned previously, a site-specific ground response analysis is usually based on 1-D equivalent-linear site response analysis (e.g., programs SHAKE and DEEPSOIL), which requires a detailed site characterization, including the information of soil profiles, layer thickness, shear-wave velocity, shear modulus, unit weight, etc. As a result, it is understood that such a site-specific analysis is aimed at examining the site effect of one particular location, instead of investigating the regional site effect in an area like the study present herein.

Therefore, the present study alike is useful to site-effect microzonation for a study area, identifying the locations within the area that should be under a higher risk with respect to site amplification or site effect. Taking this study for example, it is suggested that any development projects in those strong site-effect locations (i.e., western Taipei and the borders of the Taipei Basin) should require detailed site response analyses to thoroughly investigate the dynamic responses. Most importantly, since CAV is now being considered a better intensity measure for structure damage evaluations, the result of the study can be more useful for site-effect microzonation for the Taipei areas, providing engineers with such information for preliminary site response assessments closely related to structure safety.

5.4. Future study

This study is based on CAV to investigate the regional site effect in Taipei. As mentioned previously, CAV₂₀ was also considered a good indicator to the onset of structural damage [4], based on the comparison of CAV₂₀ to a local earthquake intensity scale in Italy. Therefore, future studies should be worth conducting to investigate site effect in terms of CAV₂₀.

Nevertheless, CAV₂₀-based studies need more strong motion data to obtain reasonable results and assessments. Taking this study for example, the majority of ground motion data were not particularly strong because of distant sources. Therefore, with a cutoff of 0.02 g, the CAV₂₀ at the reference site is equal to zero in several cases, resulting in an unrealistic, infinite amplification factor as long as the CAV₂₀ of the ground surface motion is not zero. This effect has been pointed out by Campbell and Bozorgnia [8] while they were developing CAV GMPEs. They considered CAV is relatively stable and predictable compared to others with a cutoff value, which can result in a number of zero values in an application that appears problematic, especially when it comes to

small and moderate earthquakes.

6. Summary and conclusion

Cumulative absolute velocity, CAV, is a relatively new ground motion intensity measure, and it is considered more indicative of structural damage. As a result, different from previous works this study was focused on investigating the site effect in the Taipei areas based on CAV amplification.

With the local TSMIP strong-motion database, more than 1200 strong-motion data were gathered from the database. To the best of our knowledge, such a sample size is much larger than any site-effect study of this kind, and it allows the examinations on the inevitable uncertainty of site effect that was not investigated by the previous works with limited data.

The key results of the analysis indicate that strong site effects should exist in western Taipei and in the locations close to the rims of the Taipei Basin. The result of the study is useful to the site-effect microzonation for the Taipei area, providing information to local engineers for preliminary site response assessments. Most importantly, the new CAV-based presentation should be more relevant to structure safety, considering the recent research has discovered the stronger correlation between this new intensity measure and structural damage.

Acknowledgments

We appreciate the valuable comments from the Editor and Reviewers, making the submission so much improved in so many aspects. Financial support from Ministry of Science and Technology of Taiwan (Most106–2218-E-008–013-My2) is also highly appreciated.

References

- [1] EPRI. A criterion for determining exceedance of the operating basis earthquake [Report NP-5930]. Palo Alto, California: Electric Power Research Institute; 1998.
- [2] EPRI. Standardization of the cumulative absolute velocity [Report No: TR-100082]. Palo Alto, California: Electric Power Research Institute; 1991.
- [3] Kramer SL, Mitchell RA. Ground motion intensity measures for liquefaction hazard evaluation. *Eng Spectra* 2006;22(2):413–38.
- [4] Cabañas L, Benito B, Herráiz M. An approach to the measurement of the potential structural damage of earthquake ground motions. *Earthq Eng Struct Dyn* 1997;26(1):79–92.
- [5] Campbell W, Bozorgnia Y. Cumulative absolute velocity (CAV) and seismic intensity based -on the PEER-NGA database. *Earthq Spectra* 2012;28(2):457–85.
- [6] Kostov M Site specific estimation of cumulative absolute velocity. In: *Proceeding 18th international conference on structural mechanics in reactor technology (SMiRT 18)*, Beijing, China; 2005. p. 3041–3050.
- [7] Koliopoulos PK, Margaritis BN, Klimis NS. Duration and energy characteristics of Greek strong motion records. *J Earthq Eng* 1998;2(3):391–417.
- [8] Campbell KW, Bozorgnia Y. A ground motion prediction equation for the horizontal component of cumulative absolute velocity (CAV) based on the PEER-NGA strong motion database. *Earthq Spectra* 2010;26(3):635–50.
- [9] Danciu L, Tselentis GA. Engineering ground-motion parameters attenuation relationships for Greece. *Bull Seismol Soc Am* 2007;97(1B):162–83.
- [10] EPRI. Program on technology innovation: use of cumulative absolute velocity (CAV) in determining effects of small magnitude earthquakes on seismic hazard analyses [Report No. 1014099]. Palo Alto, California: Electric Power Research Institute; 2006.
- [11] Campbell CW, Bozorgnia Y. NGA ground motion model for the geometric mean horizontal component of PGA, PGV, PGD, and 5% damped linear elastic response spectra for periods ranging from 0.01 to 10 s. *Earthq Spectra* 2008;24:139–71.
- [12] Aleik H, Ozel O, Apaydin N, Erdik M. A study on warning algorithms for Istanbul earthquake early warning system. *Seismol Res Lett* 2009;36(5). <http://dx.doi.org/10.1029/2008GL036659>.
- [13] Borchardt RD. Effect of local geology on ground motion near San Francisco Bay. *Bull Seismol Soc Am* 1979;60(1):29–61.
- [14] Kawase H. The cause of the damage belt in Kobe: “the basin-edge effect,” constructive interference of the direct S-wave with the basin-induced diffracted/Rayleigh waves. *Seismol Res Lett* 1996;67(5):25–34.
- [15] Bonilla LF, Steidl JH, Lindley GT, Tumarkin AG, Archuleta RJ. Site amplification in the San Fernando Valley, California: variability of site-effect estimation using the S-wave, Coda, and H/V methods. *Bull Seismol Soc Am* 1997;87(3):701–30.
- [16] Wen KL, Peng HY, Liu LF, Shin TC. Basin effects analysis from a dense strong motion observation network. *Earthq Eng Struct Dyn* 1995;24:1069–83.
- [17] Wen KL, Peng HY. Site effect analysis in the Taipei basin: results from TSMIP network data. *Terr Atmos Ocean Sci* 1998;9(4):691–704.
- [18] Loh CH, Hwang JY, Shin TC. Observed variation of earthquake motion across a basin – Taipei City. *Earthq Spectra* 1998;14(1):115–33.
- [19] Sokolov V, Loh CH, Wen KL. Empirical study of sediment-filled basin response: the base of the Taipei City. *Earthq Spectra* 2000;16(3):681–707.
- [20] Sokolov V, Loh CH, Wen KL. Empirical models for site-and region-dependent ground-motion parameters in the Taipei area: a Unified Approach. *Earthq Spectra* 2001;17(2):313–31.
- [21] Lee SJ, Chen HW, Liu Q, Komatsitsch D, Huang BS, Tromp J. Three-dimensional simulations of seismic-wave propagation in the Taipei basin with realistic topography based upon the spectral-element method. *Bull Seismol Soc Am* 2008;98(1):253–64.
- [22] Teng LS, Lee CT, Peng CH, Chen WF, Chu CJ. Origin and geological evolution of the Taipei basin, northern Taiwan. *West Pac Earth Sci* 2001;1(2):115–42.
- [23] Wang Y, Lee S, Ng S. “The Big One” in Taipei: numerical simulation study of the sanchiao fault earthquake scenarios. American Geophysical Union, Fall Meeting 2012; Abstract T53B-2715.
- [24] CWB. Central Weather Bureau Taiwan. Available from: <<http://www.cwb.gov.tw/V7/earthquake/acستا.htm>> [Accessed August 2017].
- [25] Shin TC, Tsai YB, Yeh YT, Liu CC, Wu YM. Strong-motion instrumentation programs in Taiwan. *Int Handb. Earthq. Eng. Seismol.* 81B. 2003. p. 1057–62.
- [26] Wen KL, Shin TC, Wu YM, Hsiao NC, Wu BR. Earthquake early warning technology progress in Taiwan. *J Disaster Res* 2009;4(4):202–10.
- [27] Kuo CH, Wen KL, Hsieh HH, Lin CM, Chang TM, Kuo KW. Site classification and Vs30 estimation of free-field TSMIP stations using the logging data of EGD. *Eng Geol* 2012;129–130:68–75.
- [28] Wu YM, Shin TC, Chang CH. Near real-time mapping of peak ground acceleration and peak ground velocity following a strong earthquake. *Bull Seismol Soc Am* 2001;91(5):1218–28.
- [29] Wu YM, Hsiao NC, Teng TL. Relationships between strong ground motion peak values and seismic loss during the 1999 Chi-Chi, Taiwan earthquake. *Nat Hazards* 2004;32(3):357–73.
- [30] Lin PS, Lee CT, Cheng CT, Sung CH. Response spectral attenuation relations for shallow crustal earthquakes in Taiwan. *Eng Geol* 2011;121(3–4):150–64.
- [31] Sokolov V, Wenzel F, Wen KL, Jean WY. On the influence of site conditions and earthquake magnitude on ground-motion within-earthquake correlation: analysis of PGA data from TSMIP (Taiwan) network. *Bull Earthq Eng* 2012;10(5):1401–29.
- [32] Wang JP, Huang D, Yang Z. Deterministic seismic hazard map for Taiwan developed using an in-house Excel-based program. *Comput Geosci* 2012;48:111–6.
- [33] Kramer SL. *Geotechnical Earthquake Engineering*. New Jersey: Prentice Hall; 1996.
- [34] Bray JD, Rathje ER. Earthquake-induced displacements of solid-waste landfills. *J Geotech Geoenviron Eng* 1998;124:242–53.
- [35] Hancock J, Bommer JJ. Using spectral matched records to explore the influence of strong motion duration on inelastic structural response. *Soil Dyn Earthq Eng* 2007;27:291–9.
- [36] Raghunandan M, Liel AB. Effect of ground motion duration on earthquake-induced structural collapse. *Struct Saf* 2013;41:119–33.
- [37] Chandramohan R, Baker JW, Deierlein GG. Quantifying the influence of ground motion duration on structural collapse capacity using spectrally equivalent records. *Earthq Spectra* 2016;32(2):927–50.
- [38] Wu YM, Yen HY, Huang BS, Liang WT. Magnitude determination using initial P waves: a single-station approach. *Geophys Res Lett* 2006;33:L05306. <http://dx.doi.org/10.1029/2005GL025395>.
- [39] Kuo CH, Wen KL, Hsieh HH, Lin CM, Chang TM. Characteristics of bear-surface S-wave velocity. Report NCREE-11-022, National Center for Research on Earthquake Engineering, Taipei, Taiwan.
- [40] Boore DM. On pads and filters: processing strong-motion data. *Bull Seismol Soc Am* 2005;95:745–50.
- [41] Loh CH. Strong motion data processing in Taiwan and its engineering application. Paper presented at invited workshop on strong-motion record processing convened by the consortium of organizations for strong-motion observation system (COSMOS), 26–27 May, COSMOS, Richmond, CA; 2004.
- [42] Boore DM, Stephens CD, Joyner WB. Comments on baseline correction of digital strong-motion data: examples from the 1999 Hector Mine, California, Earthquake. *Bull Seismol Soc Am* 2002;92:1543–60.
- [43] Converse AM, Brady AG. BAP: basic strong-motion accelerogram processing software, version 1.0, Open-File Report 92-296A, US Geological Survey; March 1992.
- [44] Wu YM, Kanamori H. Development of an earthquake early warning system using real-time strong motion signals. *Sensors* 2008;8:1–9.